Lithographic Wavelength Control of External-Cavity Laser with Silicon Photonic Crystal Cavity-based Resonant Reflector

Alexandros A. Liles,[1,*] Kapil Debnath,[1] and Liam O'Faolain[1]

[1]School of Physics and Astronomy, University of St Andrews, Scottish Universities Physics Alliance (SUPA), North Haugh, St Andrews KY16 9SS, United Kingdom
**Corresponding author: aal5@st-andrews.ac.uk*

Received XX Month XXXX; revised XX Month, XXXX; accepted XX Month XXXX; posted XX Month XXXX (Doc. ID XXXXX); published XX Month XXXX

We report the experimental demonstration of a new design for external-cavity hybrid lasers consisting of a III-V Semiconductor Optical Amplifier (SOA) with fiber reflector and a Photonic Crystal (PhC) based resonant reflector on SOI. The Silicon reflector comprises an SU8 polymer bus waveguide vertically coupled to a PhC cavity and provides a wavelength-selective optical feedback to the laser cavity. This device exhibits milliwatt-level output power and side-mode suppression ratios of more than 25 dB.

OCIS codes: *(250.0250) Optoelectronics; (050.5298) Photonic crystals; (140.5960) Semiconductor lasers.*

http://dx.doi.org/10.1364/OL.99.099999

Over the past few years, Silicon (Si) Photonics technology has emerged as a potential solution for the realization of low-cost, high performance components and Photonic Integrated Circuits (PIC) that can be used to meet the increasing bandwidth demands of chip-scale and on-chip optical interconnections [1-4]. A key feature of PICs is their ability to support Wavelength Division Multiplexing (WDM), a technique offering the parallelism necessary for high bandwidth and high density chips. Cheap, compact, efficient and Silicon compatible wavelength-tunable laser sources with precise wavelength control are thus crucial elements to facilitate the generation of WDM optical interconnects [5].

Although Silicon-On-Insulator (SOI) has proven itself to be a most appealing platform for light propagation and manipulation, practical efficient, electrically pumped lasers directly in Si or other group IV elements are still absent from the Silicon Photonics tool kit, owing to the indirect bandgap that these materials exhibit. Consequently, the use of III-V elements as gain material in lasers for WDM optical interconnects is dictated – a challenging task, as direct growth of III-V semiconductors on IV semiconductors is difficult due to lattice constant mismatch and compatibility issues.

A popular solution to the above problem is the heterogeneous integration of III-V parts on top of SOI PICs by means of direct wafer bonding [6]. An alternative approach suggests the deployment of Reflective Semiconductor Optical Amplifiers (RSOAs) and external Si-based reflectors for the formation of External-Cavity (EC) lasers. The latter approach has lately attracted significant attention as it allows independent design, fabrication and optimization of the active and the passive regions, and makes the most effective use of the III-V materials [5,7]. Up to now, devices that use Bragg gratings [7-9], ring resonators [10,11] and Sagnac interferometers [12] as Si reflectors have been demonstrated in this platform.

The concept of using grating cavity resonant mirrors for

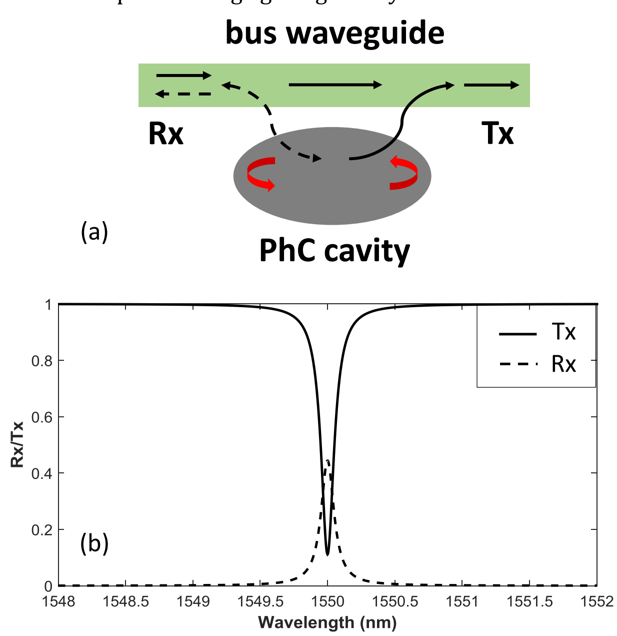

Fig. 1 (a) Conceptual representation of PhC resonator coupled to a bus waveguide at resonance. The dashed arrows represent the backwards propagating/reflected components, while the solid ones represent the forward propagating/transmitted components. (b) Reflection (Rx) and transmission (Tx) spectra of a dielectric bus waveguide coupled to a PhC cavity with $Q_{coupling} = 20000$ and $Q_{cavity} = 45000$.

heterogeneously integrated lasers has been introduced in [13, 14]. In this Letter, we present an EC laser design employing as a resonant reflector a PhC cavity coupled to a low-index waveguide [15,16], which lays the first stone towards EC laser source architectures with small footprint, high Side-Mode Suppression Ratio (SMSR), and the highly precise wavelength control required for WDM applications [5]. The Si-based reflector is simply a dielectric bus waveguide placed vertically above a Si PhC cavity, with an oxide layer between them that acts as a physical separation buffer, as described in [16]. At the resonant wavelength of the PhC cavity, light couples evanescently to the cavity mode from the waveguide mode. The functionality of the employed system as a resonant mirror stems from the optical feedback provided by the backwards propagating light component that is coupled into the bus waveguide from the PhC cavity as shown in Fig. 1(a) [13-15].

Assuming weak coupling, the transmittance and reflectance in the waveguide at resonance are given by [17]:

$$T = \frac{Q_{total}^2}{Q_{cavity}^2}; \qquad R = \frac{Q_{total}^2}{Q_{coupling}^2} \qquad \textbf{(1),}$$

where Q_{cavity} is the intrinsic Q-factor of the PhC cavity, $Q_{coupling}$ describes the coupling between the waveguide and the cavity modes, and Q_{total} is the overall Q-factor of the system, given by:

$$\frac{1}{Q_{total}} = \frac{1}{Q_{cavity}} + \frac{1}{Q_{coupling}} \qquad \textbf{(2).}$$

Fig. 1(a) shows theoretically calculated transmission and reflection spectra of a coupled PhC cavity – bus waveguide system with resonance at λ=1550 nm, $Q_{coupling} = 20000$ and $Q_{cavity} = 45000$. The vertical coupling technique allows for low insertion and transmission losses, isolation and maximization of the area available for electronic circuitry on Silicon, and offers the possibility of controlling the coupling between the bus waveguide and Si by for chip-scale optical links.

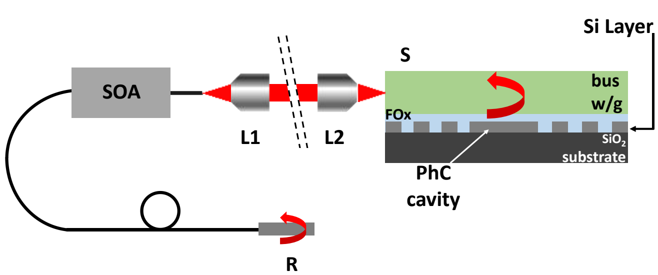

Fig. 2 Schematic representation of the proposed external cavity laser configuration and operation, comprising a fiber pigtailed SOA. R: fiber optic mirror reflector, L1, L2: objective lenses, S: sample/Si PhC cavity based mirror.

Fig 2 depicts a side-view of the EC laser configuration used. A commercially available, packaged fiber-pigtailed SOA (Kamelian OPA-20-N-C-FA with minimum fiber-to-fiber gain of 20 dB for wavelengths around 1550 nm) was used as the gain medium. A pair of objective lenses was utilized to couple the light from the SOA to the Si-reflector, by initially collimating (L1) and then focusing it (L2) on the reflector chip (S) which played the role of the first mirror of the laser cavity as described below. The second mirror is a simple fiber optic reflector (R) with reflectance R~95%. An SU8 polymer waveguide was used for the resonant reflector device described in this Letter, but the possibility of using other low-index materials has been shown [16]. The width and height of the waveguide were 3 μm and 2.1 μm respectively, resulting in low coupling losses (<3 dB/facet). A Dispersion Adapted (DA) PhC cavity [18] was vertically coupled to the SU8 bus waveguide as described in [16]. The DA design was selected due to its advantageous vertical coupling characteristics [16] and was patterned on the 220-nm SOI platform by Electron-beam Lithography and Reactive Ion Etching (RIE). Flowable Oxide (FOx-15 from Dow Corning) was used for the buffer oxide layer. The facet of the reflector chip to which the light from L2 is coupled, was AR coated to minimize back-reflections. Fabrication details for the cavity can be found in [18].

A broad IR frequency spectrum is generated by amplified spontaneous emission in the SOA and is then coupled to the SU8 waveguide. Light with wavelengths matching the resonances of the Si PhC cavity will be coupled to it from the bus waveguide and power will build up inside the cavity. Due to its nature, the Si reflector is wavelength selective, meaning that only wavelengths corresponding to the resonances of the PhC cavity are reflected backwards to the SOA. A conventional laser cavity is thus formed only for those wavelengths between the fiber reflector and the PhC cavity. As it can be seen Eq. (1) and Eq. (2), the reflectance of the Si resonant mirror can be modified at will by controlling the physical parameters of the system. The laser output is taken from the other end of the SU8 waveguide.

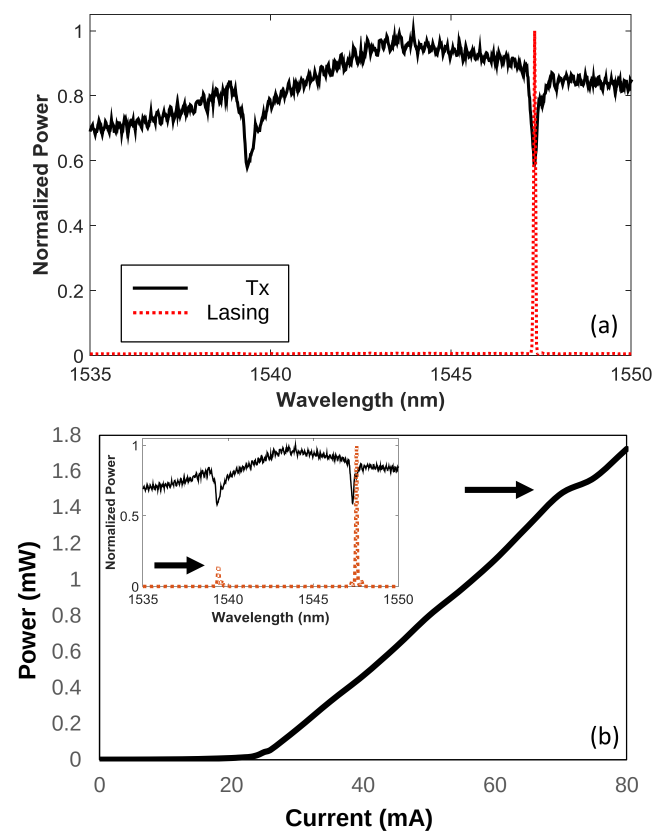

Fig. 3 Performance of a laser made with a DA PhC cavity with period lattice constant α = 388 nm and r/α = 0.28. (a) Lasing spectrum (dotted line/Lasing) showing single-mode operation at 40 mA overlaid with the transmission spectrum of an SU8 bus waveguide vertically coupled to the aforementioned DA PhC cavity (solid line/Tx). The dips in the transmission spectrum correspond to the cavity resonances. (b) L-I curve at room temperature. Inset: Lasing spectrum at 80mA (dashed line). The arrows indicate a kink in the curve attributed to the appearance of a second lasing mode caused by a higher order PhC cavity resonance.

Owing to the large length of the laser cavity (ranging from 5 to 8m, depending on the length of the fiber patchcords used) the longitudinal mode spacing is extremely narrow (sub-pm), effectively giving a longitudinal mode continuum. The lasing wavelength and linewidth are determined in this case exclusively by the PhC cavity through the above described mechanism. In this way, the proposed laser configuration is quite resilient to laser cavity length deviations, as such lasers can operate for a wide, continuous range of cavity lengths. Additionally, by fine-tuning the lattice constant of the PhC, the most precise control of the emitted wavelength (at the nm scale) in hybrid Si-III/V external cavity lasers to-date is achieved.

Lasing experiments for several PhC cavity devices were conducted at room temperature and emission at the output of the laser was collected at the end of the SU8 waveguide with a collimating lens. The collimated output was then focused by a second objective on a fiber connected to an InGaAs photodetector and an OSA for the spectral power distribution of the device under test (DUT) to be measured. Laser output spectra were taken for different values of the drive current of the SOA. The measurements were limited by the resolution of the employed OSA (0.01 nm). Figure 3(b) shows the light versus current (LI) curve measured from a laser utilizing a DA cavity with period lattice constant α = 388 nm and r/α = 0.28, as defined in [18]. The relationship between the SOA drive current and the laser output power was obtained by measuring the output power after the collimating lens with a power meter. The threshold current for the presented device was found to be 23.6 mA for lasing at 1547.32 nm, and the experimental slope efficiency was $\eta_s = 0.03236\ mW/mA$. From an analysis of the experimental threshold gain and slope efficiency a PhC cavity mirror reflectivity of ~40% and intra-cavity losses of ~7.5 dB (primarily arising from coupling losses and the non-unity mirror reflectivity) were estimated [19].

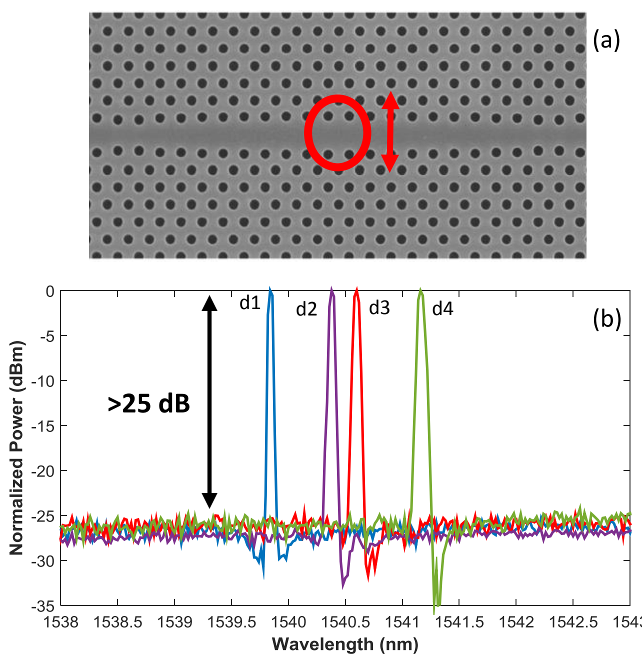

Fig. 4 (a) SEM image of a DA PhC cavity. The cavity resonant wavelengths (and thus resonant reflections) of different Si mirrors were varied by tuning the position of the four innermost holes (marked in red) of each cavity. (b) Lasing spectra for lasers utilizing reflectors based on PhC cavities with different hole shifts of the two inner pairs – d1=36 nm, d2=44 nm , d3=40 nm, d4=38 nm from the original hole position in a W1 waveguide. The extinction ratio was >25 dB for all the devices.

The kink in the LI (Fig. 3(b)) curve is caused by the appearance of a second lasing mode; DA cavities are multimodal PhC cavities, with different modes exhibiting different coupling rates to and from the bus waveguide and therefore different reflectance (R) and transmittance (T) coefficients. Each DA cavity mode can thus act as an individual reflector, resulting in the potential formation of more than one, un-coupled laser cavities (as the DA cavity modes are not coupled to each other), each with its own lasing characteristics (threshold, efficiencies etc), which share the same gain medium. For the DUT, the lasing threshold condition for the second DA cavity mode is satisfied at around 68 mA. Fig. 3(a) shows the initial single-mode operation of the examined device at 40 mA, and the existence of a second lasing mode at 80 mA (Fig. 3(b) inset). It is apparent that each mode corresponds to a PhC cavity mode, proving that the lasing wavelength in the proposed architecture is determined by the resonances of the PhC cavity. Multiple lasing modes can be avoided in various ways, the most straightforward of which, is the employment of a single-mode PhC cavity design in the suggested configuration.

As precise wavelength control is of utter importance for WDM optical links, lithographic control of the lasing wavelength was demonstrated by utilizing resonant reflectors with different PhC cavity resonances in the same configuration. The cavity resonances were tuned by varying the position of the four inner holes of the DA cavity design [18, 20], as shown in Fig. 4(a). The considered hole shifts were between 36 and 44 nm outwards, with respect to the hole position in a W1 waveguide configuration [18]. Apart from the aforementioned variation, all devices were identical. The change in the emitted wavelength from the first lasing mode of each device for 40mA drive current is shown in Fig. 4(b). The differential quantum efficiency and the slope efficiency varied in each device, depending on the reflectance of each resonant Si mirror, which in turn was determined by the coupling rate between the PhC and the SU8 waveguide. The side-mode suppression ratio was in every case high (>25 dB in Fig. 4(b)). Dynamic tuning of the wavelength emitted by the laser can be achieved by electro-optic modulation of the PhC cavity resonances [20].

In conclusion, we demonstrate for the first time a hybrid External Cavity laser architecture, comprising a fibre pigtailed SOA with a fibre optic reflector and a Si reflector based on a PhC cavity vertically coupled to a polymer (SU8) waveguide. By demonstrating a laser solution based on the vertical coupling architecture, we add to the platform previously demonstrated in [20] and [21]. The fiber-coupled arrangement is additionally attractive as the gain section is spatially separated from the wavelength selective components. In this way, the gain chip consumption does not contribute to the on-chip heat dissipation, improving the overall thermal stability of the device, which is important in many applications. Nevertheless, the lasing wavelength may still be controlled by on-chip elements (i.e. the PhC cavity) maintaining all the consequent advantages. A further reduction of the intra-cavity losses down to 3 dB can be achieved by improving the coupling losses in the set-up, leading to an increase of the slope efficiency by a factor of ~5 [19]. Moreover, the presented working principle can be extended to the butt-coupled configuration shown in [7-12]. As PhC cavities exhibit the ultimate Q/V ratio [22], they can combine ultra-small size with high FSR allowing larger spatial density and tighter frequency-channel spacing. All the above reasons render the presented device an ideal candidate for WDM interconnects.

Funding. The authors acknowledge funding from EPSRC, Scottish Enterprise and the European Research Council under Starting Grant 337509.

Acknowledgment. We thank S. Hegarty, N. K. Metzger and A. A. Gonzalez-Fernandez for fruitful discussions.

References

1. R. A. Soref, IEEE J. Sel. Top. Quantum Electron. **12**, 1678 (2006)
2. B. Jalali and S. Fathpour, J. Lightwave Technol. **24**, 4600 (2006).
3. A. V. Krishnamoorthy, R. Ho, X. Zheng, H. Schwetman, J. Lexau, P. Koka, GuoLiang Li, I. Shubin, and J. E. Cunningham, Proc. IEEE **97**, 1337 (2009)
4. Y. Vlasov, Communications Magazine IEEE **50**, s67 (2012)
5. X. Zheng, S. Lin, Y. Luo, J. Yao, G. Li, S. S. Djordjevic, J. H. Lee, H. D. Thacker, I. Shubin, K. Raj, J. E. Cunningham, and A. V. Krishnamoorthy, J. Lightwave Technol. **31**, 4142 (2013)
6. G. Roelkens, L. Liu, D. Liang, R. Jones, A. Fang, B. Koch, and J. Bowers, Laser Photon. Rev. **4**, 751 (2010)
7. A. J. Zilkie, P. Seddighian, B. J. Bijlani, W. Qian, D. C. Lee, S. Fatholoumi, J. Fong, R. Shafiiha, D. Feng, B. J. Luff, X. Zheng, J. E. Cunningham, A. V. Krishnamoorthy, and M. Ashgari, Op. Express **20**, 23456 (2012)
8. T. Creazzo, E. Marchena, S. B. Krasulick, P. K. L. Yu, D. Van Orden, J. Y. Spann, C. C. Blivin, L. He, H. Cai, J. M. Calesasse, R. J. Stone, and A. Mizrahi, Op. Express **21**, 28048 (2013)
9. S. Tanaka, S.-H. Jeong, S. Sekiguchi, T. Kurahashi, Y. Tanaka, and K. Morito, Op. Express **22**, 28057 (2012)
10. T. Chu, N. Fujioka, and M. Ishizaka, Op. Express **17**, 14063 (2009)
11. S. Lin, S. S. Djordjevic, J. E. Cunningham, I. Shubin, Y. Luo, J. Yao, G. Li, H. Thacker, J.-H. Lee, K. Raj, X. Zheng, and A. V. Krishnamoorthy, Op. Express **21**, 32425 (2013)
12. Y. Zhang, S. Yang, H. Guan, A. E.-J. Lim, G.-Q. Lo, P. Magill, T. Baehr-Jones, and M. Hochberg, Op. Express **22**, 17872 (2014)
13. Y. De Koninck, F. Raineri, A. Bazin, R. Raj, G. Roelkens, and R. Baets, Op. Lett. **38**, 2496 (2013)
14. Y. De Koninck, G. Roelkens, and R. Baets, Laser Photon. Rev. **9**, L6 (2015)
15. M. Qiu, Op. Lett. **30**, 1476 (2005)
16. K. Debnath, K. Welna, M. Ferrera, K. Deasy, D. G. Lidzey, and L. O'Faolain, Op. Lett. **38**, 154 (2013)
17. Y. Xu, Y. Li, R. K. Lee, and A. Yariv, Phys. Rev. E **62**, 7389 (2000)
18. K. Welna, S. L. Portalupi, M. Galli, L. O'Faolain, and T. F. Krauss, IEEE J. Quant. Electron. **48**, 1177 (2012)
19. L. A. Coldren, S. W. Corzine, M. L. Mashanovitch, Diode lasers and photonic integrated circuits - 2nd Edition, (Wiley, New York, 2012)
20. K. Debnath, L. O' Faolain, F. Y. Gardes, A. G. Steffan, G. T. Reed, and T. F. Krauss, Op. Express **20**, 27420 (2012)
21. K. Debnath, F. Y. Gardes, A. P. Knights, G. T. Reed, T. F. Krauss, L. O'Faolain, App. Phys. Lett. **102**, 171106 (2013)
22. M. Notomi, K. Nozaki, A. Shinya, S. Matsuo, and E. Kuramochi, Opt. Commun. **314**, 3 (2014)

References

1. R. A. Soref, "The past, present and future of silicon photonics", IEEE J. Sel. Top. Quantum Electron., 12(6), 1678-1678 (2006)
2. B. Jalali and S. Fathpour, "Silicon photonics," J. Lightwave Technol. 24(12), 4600–4615 (2006).
3. A. V. Krishnamoorthy, R. Ho, X. Zheng, H. Schwetman, J. Lexau, P. Koka, GuoLiang Li, I. Shubin, and J. E. Cunningham, "Computer systems based on silicon photonic interconnects," Proc. IEEE 97(7), 1337–1361 (2009)
4. Y. Vlasov, "Silicon CMOS-integrated nano-photonics for computer and data communications beyond 100G," Communications Magazine IEEE 50, s67–s72 (2012)
5. X. Zheng, S. Lin, Y. Luo, J. Yao, G. Li, S. S. Djordjevic, J. H. Lee, H. D. Thacker, I. Shubin, K. Raj, J. E. Cunningham, and A. V. Krishnamoorthy, "Efficient WDM laser sources towards terabyte/s silicon photonic interconnects," J. Lightwave Technol. 31(24), 4142–4154 (2013)
6. G. Roelkens, L. Liu, D. Liang, R. Jones, A. Fang, B. Koch, and J. Bowers, "III-V/silicon photonics for on-chip and intra-chip optical interconnects", Laser Photon. Rev. 4, 751-779 (2010)
7. A. J. Zilkie, P. Seddighian, B. J. Bijlani, W. Qian, D. C. Lee, S. Fatholoumi, J. Fong, R. Shafiiha, D. Feng, B. J. Luff, X. Zheng, J. E. Cunningham, A. V. Krishnamoorthy, and M. Ashgari"Power-efficient III-V/Silicon external cavity DBR lasers", Op. Express 20, Issue 21, pp 23456-23462 (2012)
8. T. Creazzo, E. Marchena, S. B. Krasulick, P. K. L. Yu, D. Van Orden, J. Y. Spann, C. C. Blivin, L. He, H. Cai, J. M. Calesasse, R. J. Stone, and A. Mizrahi, "Integrated tunable CMOS laser", Op. Express 21, Issue 23, pp 28048-28053 (2013)
9. S. Tanaka, S.-H. Jeong, S. Sekiguchi, T. Kurahashi, Y. Tanaka, and K. Morito, "High-output-power, single-wavelength silicon hybrid laser using precise flip-chip bonding technology", Op. Express 22, Issue 27, pp 28057-28069 (2012)
10. T. Chu, N. Fujioka, and M. Ishizaka, "Compact, lower-power-consumption wavelength tunable laser fabricated with silicon photonic-wire waveguide micro-ring resonators", Op. Express 17, Issue 16, pp 14063-14068 (2009)
11. S. Lin, S. S. Djordjevic, J. E. Cunningham, I. Shubin, Y. Luo, J. Yao, G. Li, H. Thacker, J.-H. Lee, K. Raj, X. Zheng, and A. V. Krishnamoorthy, "Vertical-coupled high-efficiency tunable III-V-CMOS SOI hybrid external-cavity laser", Op. Express 21, Issue 26, pp 32425-32431 (2013)
12. Y. Zhang, S. Yang, H. Guan, A. E.-J. Lim, G.-Q. Lo, P. Magill, T. Baehr-Jones, and M. Hochberg, "Sagnac loop mirror and micro-ring based laser cavity for silicon-on-insulator", Op. Express 22, Issue 15, pp 17872-17879 (2014)
13. Y. De Koninck, F. Raineri, A. Bazin, R. Raj, G. Roelkens, and R. Baets, "Experimental demonstration of a hybrid III-V-on-silicon microlaser based on resonant grating cavity mirrors", Op. Lett. 38, Issue 14, pp 2496-2498 (2013)
14. Y. De Koninck, G. Roelkens, R. Baets, " Electrically pumped 1550 nm single mode III-V-on-silicon laser with resonant grating cavity mirrors", Laser Photon. Rev. 9, Issue 2, pp L6-L10 (2015)
15. M. Qiu, "Vertically coupled photonic crystal optical filters", Op. Lett. 30, Issue 12, pp 1476-1478 (2005)
16. K. Debnath, K. Welna, M. Ferrera, K. Deasy, D. G. Lidzey, and L. O'Faolain, "Highly efficient optical filter based on vertically coupled photonic crystal cavity and bus waveguide", Op. Lett. 38, Issue 2, pp 154-156 (2013)
17. Y. Xu, Y. Li, R. K. Lee, and A. Yariv, "Scattering-theory analysis of waveguide-resonator coupling", Phys. Rev. E 62, No 5, pp 7389-7404 (2000)
18. K. Welna, S. L. Portalupi, M. Galli, L. O'Faolain, and T. F. Krauss, "Novel dispersion-adapted photonic crystal cavity with improved disorder stability", IEEE J. Quant. Electron. 48, No 9, pp 1177-1183 (2012)
19. L. A. Coldren, S. W. Corzine, M. L. Mashanovitch, "Diode lasers and photonic integrated circuits", 2nd Edition, Wiley, New York (2012)
20. K. Debnath, L. O' Faolain, F. Y. Gardes, A. G. Steffan, G. T. Reed, and T. F. Krauss, "Cascaded modulator architecture for WDM applications", Op. Express 20, Issue 25, pp 27420-27428 (2012)
21. K. Debnath, F. Y. Gardes, A. P. Knights, G. T. Reed, T. F. Krauss, L. O'Faolain, "Dielectric waveguide vertically coupled to all-silicon photodiodes operating at telecommunication wavelengths", App. Phys. Lett. 102, Issue 17, No 171106 (2013)
22. M. Notomi, K. Nozaki, A. Shinya, S. Matsuo, and E. Kuramochi, "Toward fJ/bit optical communication in a chip", Opt. Commun. 314, pp 3-17 (2014)